2022

Evaporator Flooding upon Compressor Start-up as a Function of Heat Exchanger Geometry and Refrigerant

Smrithi Pranatharthi Haran

Leon P. M. Brendel

Haotian Liu

James E. Braun

Eckhard A. Groll

Evaporator Flooding upon Compressor Start-up as a Function of Heat Exchanger Geometry and Refrigerant

Smrithi PRANATHARTHI HARAN, Leon P.M. BRENDEL, Haotian LIU, James E. BRAUN, Eckhard A. GROLL

Ray W. Herrick Laboratories, School of Mechanical Engineering, Purdue University
West Lafayette, 47907-2099, USA

pranatha@purdue.edu, brendel@purdue.edu, liu1460@purdue.edu, jbraun@purdue.edu, groll@purdue.edu

ABSTRACT

The dangers of liquid flooding in compressors are well known, yet the conditions during startup that can lead to refrigerant exiting an evaporator and thus entering a compressor are poorly understood. This research investigates how different refrigerants and heat exchanger geometries affect the severity of flooding during transients associated with compressor start up. R134a, R1234ze(E), R245fa, and R404A were tested in three heat exchangers with internal volumes of 0.12, 0.21, and 0.46 liters. A refrigerant charge threshold below which flooding never occurred was determined for each heat exchanger and each refrigerant, which increased with the size of the heat exchanger and with decreasing viscosity. Additionally, the time from the onset till the end of flooding at the evaporator outlet was visually determined for each test run. This duration of flooding generally increased with increasing charge levels and with higher kinematic viscosity and surface tension when comparing refrigerants in the same evaporator. At high charge levels, any one refrigerant showed the flooding time for a given charge regardless of the heat exchanger geometry.

Keywords: Vapor compression cycle, two-phase flow, start-up, liquid flooding, slugging, sloshing

1. INTRODUCTION

Vapor compression refrigeration cycles leverage the heat of evaporation to provide cooling. The refrigerant should be gaseous when leaving the evaporator to protect the compressor from liquid ingestion. A liquid phase exiting the evaporator is defined as 'liquid flooding' or 'flooding' in this paper. Liquid flooding may occur at cycle start-up if a large portion of the refrigerant sits in the evaporator. When the compressor starts, the pressure pull-down may cause flashing of the liquid phase and thereby flooding of liquid out of the evaporator and into the compressor.

Positive displacement compressors have a fixed volume ratio, and the introduction of an incompressible liquid could cause damage or complete failure. This reasoning is supported for example by Laughman et al. (2006), claiming that liquid flooding is "one of the most common causes of failure in reciprocating compressors". Singh et al. (1968) concluded that the cylinder pressure can be ten times the peak pressure under normal operational conditions given the presence of liquid. Siewert (1972) additionally states that these high pressures due to liquid flooding at start-up "will result in physical destruction" of many internal parts of the compressor. However, Liu and Soedel (1995) state that the pressure can only reach a destructive magnitude if the compression chamber is filled with liquid at any point during the compression process. Another concern stated by Breuker and Braun (1998) is that oil may be carried out of the compressor shell if liquid refrigerant is present in the compressor at start-up. Generally, the open literature specifically on flooding from the evaporator upon compressor start-up is very scarce.

Beck et al. (2021) initiated research on this topic and found that the occurrence of flooding at compressor start-up strongly depends on the amount of refrigerant in the evaporator at the moment of compressor start-up. Below a certain

amount of charge, flooding was never recorded. Beck et al. (2021) also compared the flooding threshold for the evaporator in the horizontal and vertical orientation but found only small differences. Brendel et al., (2022) investigated the flooding thresholds in normal versus microgravity environments and found only small differences, too. Hence, neither orientation nor absolute gravitational acceleration had strong impacts on the flooding thresholds for the tested heat exchangers.

This work continues the experimental investigation in normal gravity with three additional refrigerants and two additional heat exchangers in the vertical orientation.

2. TEST STAND AND METHODOLOGY

2.1 Experimental Set-up

The migration of liquid to the outlet of an evaporator at start-up is a highly transient, dynamic, and partially random process. Therefore, the test stand to investigate and quantify any related phenomena required a design enhancing the repeatability of the flooding observations. This was achieved by connecting a refrigerant tank to a heat exchanger, also called the 'test section' via a ball valve. The amount of refrigerant charged to the heat exchanger was measured in the tank with a liquid level probe and the ball valve was fully closed after charging the test section. This procedure meant that the evaporator inlet was fully closed during test execution in the experiment, while in a normal cycle operation the refrigerant is continuously replenished. Hence, the experiment was designed by trading off repeatability with a realistic cycle start-up. A recovery pump was used as the compressor and pushed refrigerant from the heat exchanger back into the tank when it was turned on. A transparent sight tube at the outlet of the test section allowed the operator to observe if liquid exited the evaporator during a test run. The total time of liquid in the sight tube was measured and called the 'elapsed time of liquid flooding'. An uncertainty of +/-1 s was estimated for this measurement equivalent to Beck et al. (2021), who used an earlier version of the presented test stand. Additionally, three pressure transducers were used in the setup. One of them was used to measure the tank pressure. Another one was used to measure the pressure at the inlet of the heat exchanger and was placed directly after the ball valve connecting the tank and that heat exchanger. The last one was placed at the outlet of the heat exchanger to measure a possible pressure differential across the heat exchanger during test execution. Figure 1 shows a schematic and Figure 2 shows a picture of the test stand.

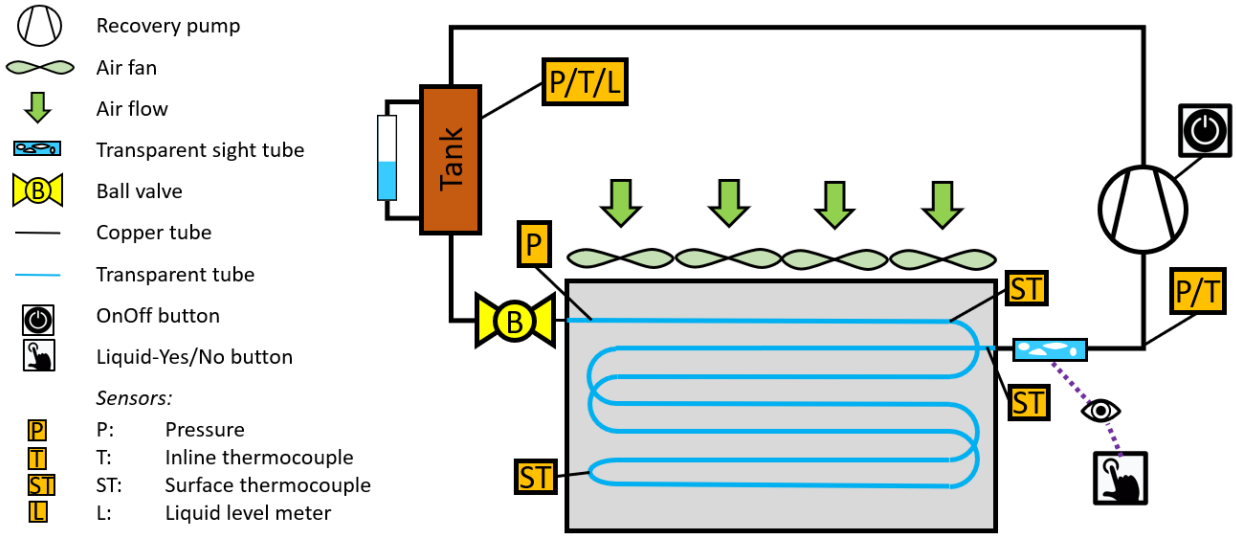

Figure 1: Schematic of the start-up test stand used for experimentation

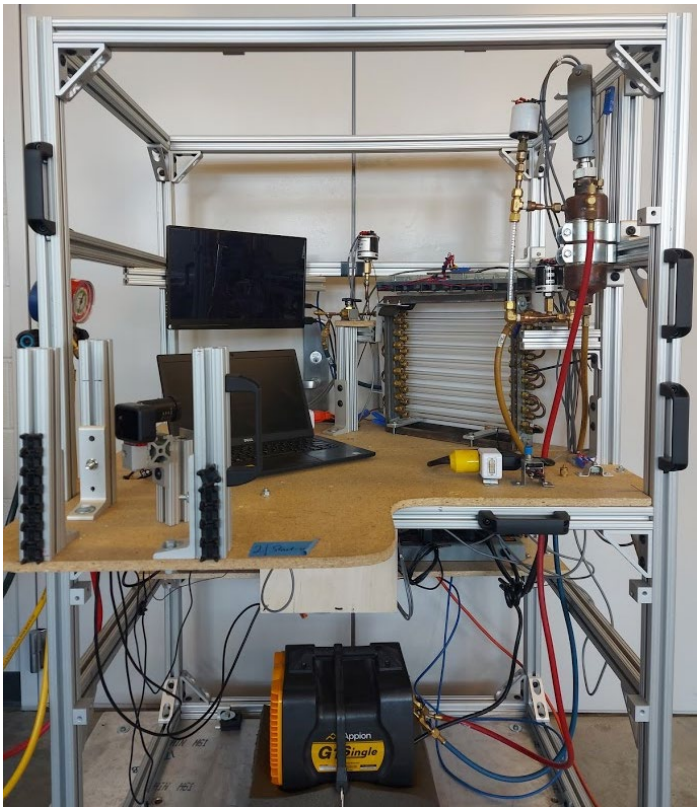

Figure 2: The test-stand used for this investigation

2.2 Test Stand Operation

A test run started with the recovery pump turned off and pressure below 70 kPa in the test section ensuring no liquid phase and therefore a negligible mass of refrigerant. The test section was then charged with refrigerant from the tank by opening the ball valve and monitoring the liquid level probe reading. The ball valve was closed after a desired amount of charge had entered the evaporator. Then, the recovery pump was turned on while visually inspecting the sight tube for liquid flooding. If 'liquid' was observed, the operator pressed a push-button until there was no more liquid refrigerant visible. The signal of the push button was recorded by the data acquisition system and converted to an elapsed time of flooding. If flooding stopped and restarted, the total time of the separate liquid occurrences was calculated.

2.3 Refrigerants under Analysis

To understand how thermophysical properties of different refrigerants affected the flooding, R134a, R1234ze(E), R245fa, and R404A were chosen. R134a was used as a baseline since it was also used by Brendel et al., (2022) and Beck et al. (2021). R1234ze(E) was used to verify that minor differences in kinematic viscosity, density, and surface tension lead to similar flooding behaviors. R245fa was chosen for its starkly higher kinematic viscosity, density, and surface tension than R134a and R1234ze(E) and its lower saturation pressure at a given temperature. In contrast, R404A was chosen for its lower kinematic viscosity, density, and surface tension than the other refrigerants tested and its higher saturation pressure. Table 1 shows the refrigerants with their safety classification and saturation pressure at 20°C. Figure 3 shows the density, kinematic viscosity of the liquid phase, and the surface tension of the four refrigerants for a range of temperatures. Refrigerant properties were calculated with EES (Klein & Alvarado, 2002) and CoolProp (Bell et al., 2014).

Table 1: Refrigerant selection and pressures at 20ºC for refrigerants chosen

Refrigerant	Safety Group Classification	Pressure [kPa] @20ºC
R245fa	B1 [Toxic | No Flame Propagation]	122.4
R134a	A1 [No Flame Propagation]	572.1
R1234ze(E)	A2L [Low Flammability]	429.0
R404A	A1 [No Flame Propagation]	1090.8

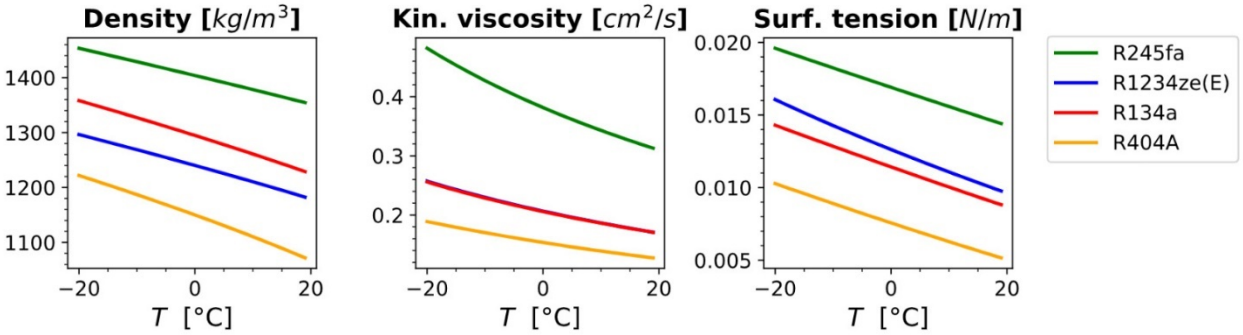

Figure 3: Relationship between kinematic viscosity and surface tension with respect to temperature for the four refrigerants. The kinematic viscosities of R134a and R1234ze(E) are almost equivalent such that the lines overlap.

2.4 Heat Exchanger Geometries

Three heat exchangers with varying volumes and numbers of tubes were chosen to understand the effects of geometrical parameters on the flooding process. Figure 4 shows the three heat exchangers where the left picture represents two heat exchangers. By changing a u-bend of the transparent heat exchanger, indicated by the red circle, the heat exchanger was decreased in size. These two configurations were called the 'medium' and 'small' heat exchanger. The picture on the right shows the third heat exchanger geometry used for this investigation called the 'large' evaporator. A transparent tube was attached to the outlet as shown in the picture to enable the detection of liquid flooding.

Table 2 shows the main physical differences between the heat exchangers. The internal volume values were calculated by charging the system with a known amount of gaseous R134a. Using temperature and pressure to calculate the density, the volume of the test section was found.

The table also shows other key geometrical differences between the heat exchangers, which include the internal diameters of the tubing and the 'height', which was measured from the top tube of the heat exchanger to the mounting board. The visual inspection of flooding from the large evaporator was more difficult for the operator than for the two other evaporators because refrigerant could not be observed inside the heat exchanger as it migrated towards the outlet and because the inner diameter of the sight tube was smaller leading to a slightly larger uncertainty in the signal for liquid flooding.

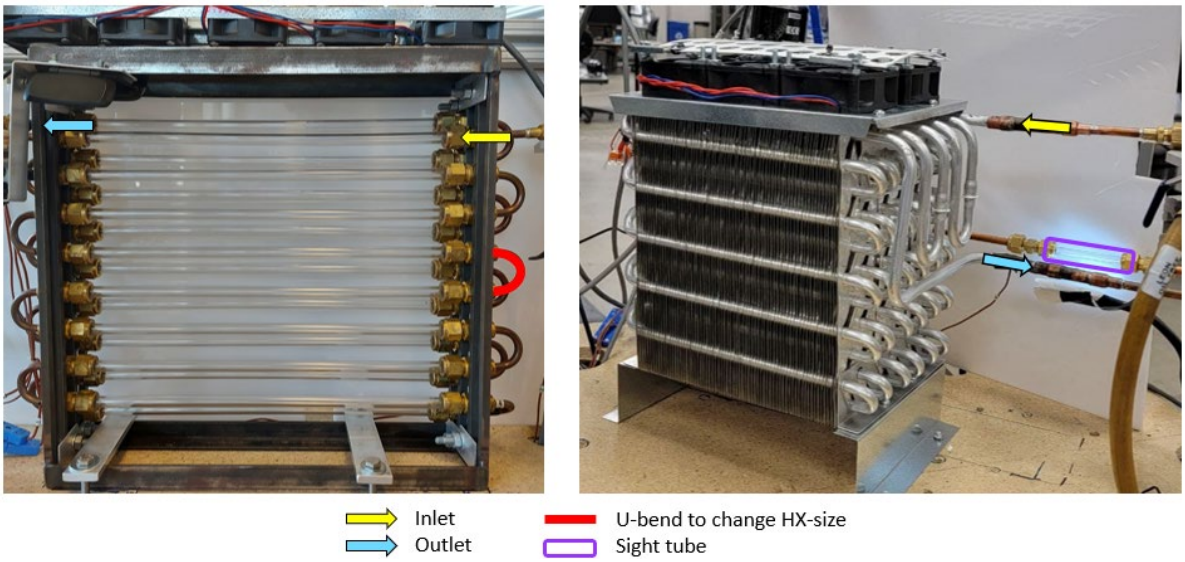

Figure 4: Heat exchangers used for the experiment. Transparent evaporator medium (1) or small (2) depends on u-bend placement (left). Large aluminum metal (3) evaporator (right).

Table 2: Physical properties of the three heat exchanger geometries used for experimentation.

Properties	**Heat Exchanger Geometries**		
	Small	**Medium**	**Large**
Material	Polycarbonate	Polycarbonate	Aluminum
Volume [liters]	0.1152	0.2109	0.4648
Outer tube diameter [mm]	9.5	9.5	7.9
Inner tube diameter [mm]	6.35	6.35	6.18
Height [cm]	16.5	33	27 (including 6 cm gap)
Length of individual tubes [cm]	41.5	41.5	24.5
Length of coil [m]	3.94	7.44	17.78
Number of tubes	9	17	22 (23 with sight glass)
Number of rows/columns	4-5 rows/ 2 cols	8-9 rows/ 2 cols	11 rows / 6 cols
Outer diameter of sight tube [mm]	9.5	9.5	6.35
Distance (sight glass and outlet) [cm]	0	0	33
Fin Spacing [cm]	None	None	0.25 cm
Number of fins	0	0	70

The circuiting of the three heat exchangers is shown in Figure 5 where the black arrows indicate the flow direction. In the transparent evaporators, the refrigerant traveled down and up once while this occurred three times in the large evaporator. For the large evaporator, the tubes had a staggered arrangement that is not depicted in the schematic.

All heat exchangers were exposed to an ambient airflow. After a test run, this airflow warmed up the body of the heat exchanger faster than the sight tube for the large evaporator. As a result liquid refrigerant sometimes condensed in the outlet tube after charging and before starting the pump. This led to a very early but short initial occurrence of liquid before flooding from the body of the heat exchanger started. However, this had only a small effect on the total time of flooding.

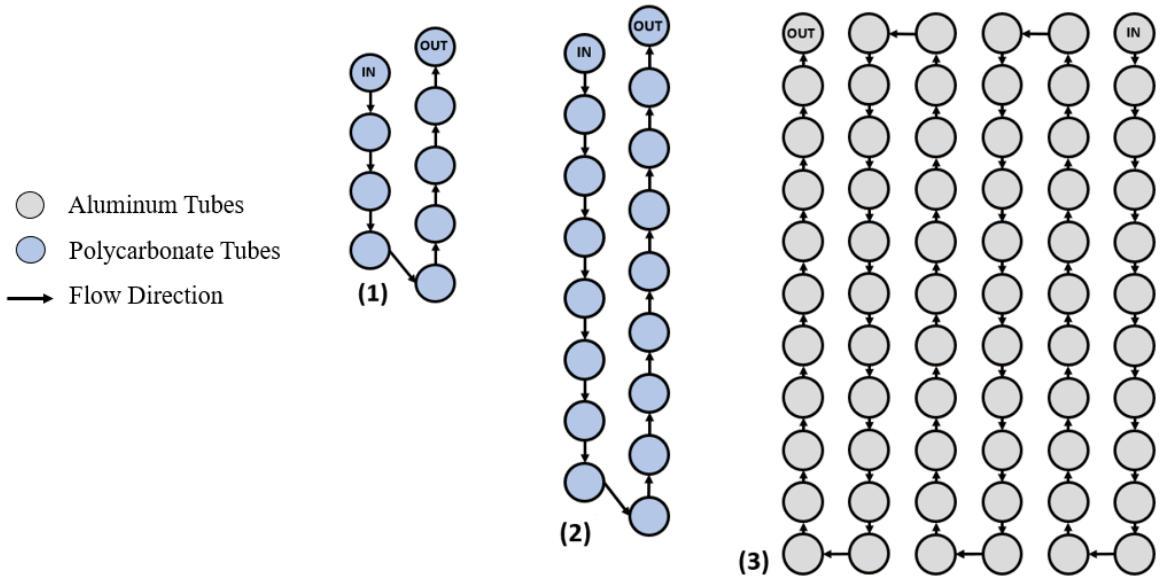

Figure 5: Tube arrangement in the cross-sectional view of all heat exchangers used. (1) Medium evaporator [left], (2) small evaporator [center], (3) large evaporator [right]

2.5 Available Data

Table 3 shows the number of data points collected for each refrigerant in each heat exchanger geometry. Datapoints were removed in post-processing if they were clearly impacted by human error, for example accidentally hitting or releasing the push button that indicates liquid flooding.

An uncertainty in this investigation was the influence of the tank temperature on the calculated charge values. During testing, the tank heats up from ambient temperature to some equilibrium temperature at continuous testing, typically around 35° C. Due to thermal expansion, the same mass of refrigerant in the tank will then have a higher liquid level. The liquid level probe is not calibrated for varying temperatures to account for this. The data was hence post-processed to account for this uncertainty by comparing the mass of the refrigerant at 20°C and the temperature of the tank at the beginning of a test run.

Table 2: Number of clean data points collected for each refrigerant-heat exchanger combination

	Small	**Medium**	**Large**
R134a	21	56	43
R1234ze(E)	19	55	37
R245fa	16	43	27
R404A	26	38	29

3. RESULTS

3.1 General trend of measurements

Figure 6 shows results for the elapsed time of flooding of R134a in the medium evaporator as a function of the initial charge. At low charges, no liquid flooding was observed. Consequently, the plot shows that the duration of flooding was zero at low initial refrigerant charges below about 50 g and then experienced a step-change in the elapsed time. This characteristic curve was also found by Beck et al. (2021) using a similar test setup.

The minimum initial charge at which flooding occurs is defined as the charge *threshold*. Further increasing the initial charge values resulted in prolonged liquid flooding at the outlet of the evaporator. This is reflected in Figure 6 with

an approximately linear relationship between the duration of flooding and the initial charge for refrigerant charges > 50 g.

The scatter in the results is not immediately explainable. Human error or a large uncertainty inherent to the type of testing is possible. However, both cannot explain that there was less scatter for R1234ze(E) and R404A as can be seen in the following sections, but maybe because R134a was the first refrigerant to be tested.

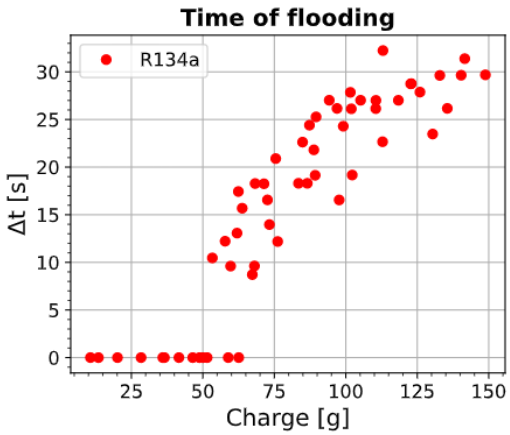

Figure 6: Duration of flooding for each refrigerant with respect to the initial charge of R134a in the medium heat exchanger

3.2 Trends with Different Refrigerants

Figure 7 shows the elapsed time of flooding for all four tested refrigerants for the medium heat exchanger. All four refrigerants had different threshold charge levels below which no liquid flooding was observed. R245fa had the lowest threshold followed by R1234ze(E), R134a, and R404A (disregarding one outlier of R1234ze(E) at ≈ 39g). The same order was found when observing the duration of liquid flooding at any given charge value. All the refrigerants had a linear trend for the duration of liquid flooding for charge values beyond their respective thresholds. R245fa had both the longest flooding time and the steepest gradient in the linear trend.

The flooding duration increased with the refrigerants in the order R245fa, R1234ze(E), R134a, and R404A. This is also the order of decreasing kinematic viscosity and surface tension as shown in Figure 3. This suggests a correlation of the flooding behavior with the thermophysical properties of the refrigerant. The flooding threshold for R245fa and R1234ze(E) seem to be similar and the lowest, followed by increasing viscosity by R134a and then R404A.

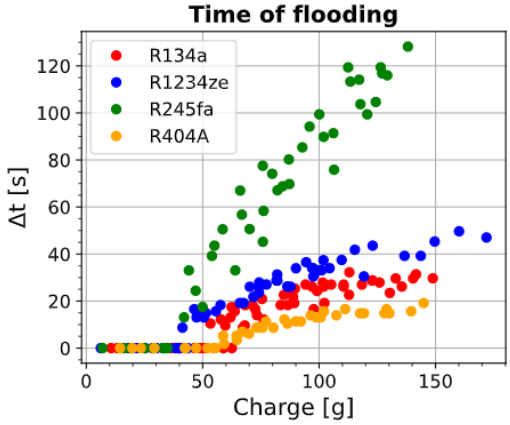

Figure 7: Duration of flooding for each refrigerant with respect to the initial charge of refrigerant in the medium heat exchanger

The open literature does not discuss any correlation of flooding intensity with viscosity or other thermophysical properties, but a hypothesis can be proposed: Upon compressor start-up, vapor bubbles are formed in the liquid phase of the refrigerant in the heat exchanger. In viscous fluids with high surface tensions, their shape and path of movement are less flexible than in fluids of low viscosity and surface tension. Therefore, the generated bubbles push more liquid towards the outlet as they grow in size. In fluids of low viscosity, the bubbles can pass by the liquid towards the outlet without moving the liquid as much. This could explain, that for higher viscosity fluids, smaller initial charge levels lead to flooding. The longer elapsed times of flooding could be explained with lower flow velocities at the higher viscosities. However, these hypotheses are far from validated.

3.3 Trends with Different Heat Exchanger Geometries

Figure 8 shows the elapsed time of flooding for each refrigerant in the three different heat exchangers. R245fa was plotted with a different y-scale to accommodate all data points. For each refrigerant, the flooding threshold increased with the size of the heat exchanger. While a correlation with size is intuitive, it is unclear whether the primary dependence lies in the internal volume, coil length, tube diameter, heat exchanger height, or the number of tubes and bends.

Although different geometries had different threshold charge values, the flooding times for a given initial charge converged for all three heat exchangers at high charge levels. A mechanistic relationship for the flooding threshold or time as a function of geometric parameters would be desirable but is beyond the scope of this paper and no relevant derivations were found in the open literature.

Overall, the geometry had a much larger effect on the threshold charge than the thermophysical properties for the combinations tested, while the thermophysical properties had a greater influence on the duration of flooding than the geometry. For any given refrigerant, the heat exchanger geometry caused threshold differences between 50 (R245fa) and 100 g (R404A). In contrast, for the large evaporator, the threshold of the four refrigerants differed by only 15 g.

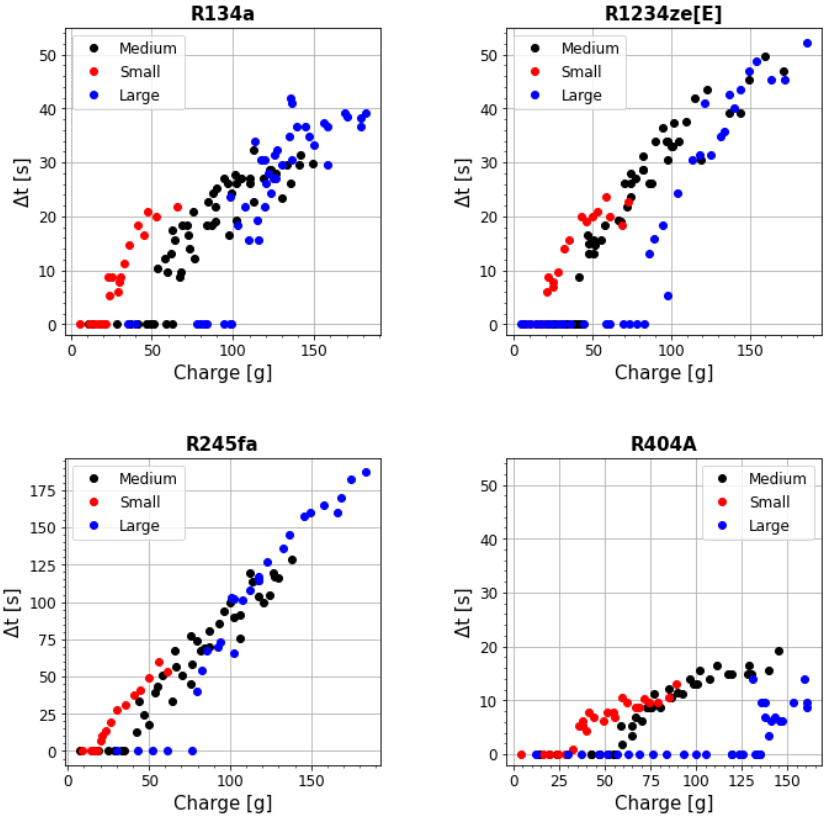

Figure 8: Duration of flooding for each refrigerant with respect to the initial charge of refrigerant in the medium heat exchanger (black), small heat exchanger (red), and large heat exchanger (blue)

4. DISCUSSION

The results show a clear dependence of the flooding behavior on refrigerants and heat exchanger geometries. However, it is important to draw attention to the uncertainties of this investigation.

The liquid flooding detection was dependent on human observation, an uncertainty not exactly quantifiable. A potential improvement to the test stand design could be to use a motion detection sensor at the transparent outlet of the heat exchanger. However, liquid flooding typically ends by fading very slowly. The liquid is then visible at the bottom of the tube, but no waves or other visible motion exists. It is unlikely that a motion detector could detect the end of flooding more accurately than a human.

No theoretical relationship was found in the literature for the intensity of flooding from an evaporator upon compressor start-up. Future research should seek a more mechanistic relationship to explain the experimental results. Possibly a dimensionless or dimensional constant could be found that better predicts when flooding starts to occur than the threshold charge that was used for this analysis.

5. CONCLUSIONS

The conditions that lead to liquid flooding from an evaporator upon compressor start-up are only scarcely discussed in the open literature. This investigation presented experimental flooding data for refrigerants with varying thermophysical properties and heat exchanger geometries. The results show a clear effect of these two factors on the duration of flooding. Key conclusions are drawn as follows:

- The higher the kinematic viscosity of a refrigerant, the lower its threshold charge for the onset of flooding for a given heat exchanger geometry.
- The smaller the size of a heat exchanger, the lower the threshold charge for a given refrigerant. It remains unclear what the most suitable measure for size is (coil length, internal volume, internal diameter, etc.).
- The different sizes affected the threshold more than the different refrigerants in this study.
- For relatively high charge levels, the elapsed time of flooding converges across different heat exchangers for a given refrigerant and diverges for different refrigerants in one heat exchanger

A mechanistic relationship of the flooding threshold and duration as a function of thermophysical properties and heat exchanger geometries is suggested for future work.

NOMENCLATURE

T	temperature	(C)
t	time	(s)
Δ	change in	(-)
Charge	mass of refrigerant	(g)

REFERENCES

Beck, P. E., Brendel, L. P. M., Braun, J. E., & Groll, E. A. (2021). *Investigation of Two-phase Refrigerant Behavior Upon Cycle Startup for Compressor Protection in Microgravity Applications*. International Refrigeration and Air Conditioning Conference.

Bell, I. H., Wronski, J., Quoilin, S., & Lemort, V. (2014). Pure and Pseudo-pure Fluid Thermophysical Property Evaluation and the Open-Source Thermophysical Property Library CoolProp. *Industrial & Engineering Chemistry Research*, *53*(6), 2498–2508. https://doi.org/10.1021/ie4033999

Brendel, L. P. M., Beck, P. E., Caskey, S. L., Ore, J. P., Braun, J. E., & Groll, E. A. (2022). Liquid Flooding from an Evaporator upon Compressor Start-up in Microgravity. *Journal of Microgravity Science and Technology*.

Breuker, M., & Braun, J. (1998). Common Faults and Their Impacts for Rooftop Air Conditioners. *HVAC&R Research*, *4*(3), 303–318. https://doi.org/10.1080/10789669.1998.10391406

Klein, S. A., & Alvarado, F. L. (2002). *Engineering Equation Solver (EES)* (V10.643) [Computer software]. F-Chart Software. http://fchartsoftware.com/ees/

Laughman, C. R., Armstrong, P. R., Norford, L. K., & Leeb, S. B. (2006). *The Detection of Liquid Slugging Phenomena in Reciprocating Compressors via Power Measurements*. International Compressor Engineering Conference at Purdue,.

Liu, Z., & Soedel, W. (1995). A Mathematical Model for Simulating Liquid and Vapor Two-Phase Compression Processes and Investigating Slugging Problems in Compressors. *HVAC&R Research*, *1*(2), 99–109. https://doi.org/10.1080/10789669.1995.10391312

Siewert, H. G. (1972). *Compressor Tolerance to Liquid Refrigerant*. International Compressor Engineering Conference, West Lafayette, IN, USA.

Singh, R., Nieter, J. J., & Prater, G. (1968). *Prediction of Slugging-Induced Cylinder Overpressures*. International Compressor Engineering Conference.